BIOCHEMISTRY
including biophysical chemistry & molecular biology

Article

pubs.acs.org/biochemistry

Reining in Polyoma Virus Associated Nephropathy: Design and Characterization of a Template Mimicking BK Viral Coat Protein Cellular Binding

Christopher O. Audu,[†] Bethany O'Hara,[§] Maria Pellegrini,[†] Lei Wang,[‡] Walter J. Atwood,[§] and Dale F. Mierke*[,†]

[†]Department of Chemistry, Dartmouth College, Hanover, New Hampshire 03755, United States

[‡]Laboratory of Physical Chemistry, ETH Zurich, 8093 Zurich, Switzerland

[§]Department of Molecular Biology, Cell Biology & Biochemistry, Brown University, Providence, Rhode Island 02912, United States

Supporting Information

ABSTRACT: The BK polyoma virus is a leading cause of chronic post kidney transplantation rejection. One target for therapeutic intervention is the initial association of the BK virus with the host cell. We hypothesize that the rate of BKV infection can be curbed by competitively preventing viral binding to cells. The X-ray structures of homologous viruses complexed with N-terminal glycoproteins suggest that the BC and HI loops of the viral coat are determinant for binding and thereby infection of the host cell. The large size of the viral coat precludes it from common biophysical and small molecule screening studies. Hence, we sought to develop a smaller protein template incorporating the identified binding loops of the BK viral coat in a manner that adequately mimics the binding characteristics of the BK virus coat protein to cells. Such a mimic may serve as a tool for the identification of inhibitors of BK viral progression. Herein, we report the design and characterization of a reduced-size and soluble template derived from a four-helix protein—TM1526 of *Thermatoga maritima* archaea bacteria—which maintains the topological display of the BC and HI loops as found in the viral coat protein, VP1, of BKV. We demonstrate that the GT1b and GD1b sialogangliosides, which bind to the VP1 of BKV, also associate with our BKV template. Employing a GFP-tagged template, we show host cell association that is dose dependent and that can be reduced by neuraminidase treatment. These data demonstrate that the BKV template mimics the host cell binding observed for the wild-type virus coat protein VP1.

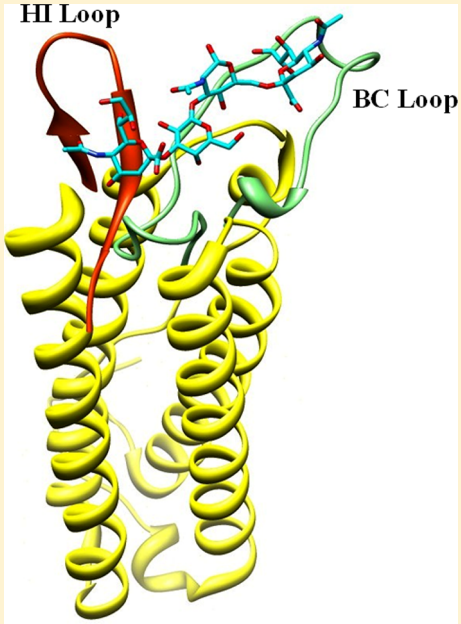

The BK virus, named after the first patient from which the virus was isolated[26] and a member of the polyoma viral family with double-stranded DNA, is the leading cause of polyoma virus associated nephropathy (PVAN)—resulting in chronic post kidney transplantation rejection—and hemorrhagic cystitis in bone marrow transplantation patients.[1−4] While a high percentage (80%) of the population harbors the virus, its mode of infection is currently not known.[3] Following infection at an early age, a state of latency is established in renal tubular epithelial and urothelial cells. Reactivation is associated with immuno-compromised conditions, and in particular PVAN tends to arise with the use of pro-transplant drugs including tacrolimus (a calcineurin inhibitor and, thus, an IL-2 suppressant) and mycophenolate mofetil—a purine synthesis inhibitor.[5,6] Current treatment of PVAN has centered on early diagnosis and reduction in dosages of the immunosuppressants. Leflunomide, a pyrimidine synthesis inhibitor, and cidofovir, a nucleoside analogue, are also being used to treat PVAN with mixed results.[7−9] The use of nucleoside analogues, such as gancyclovir or cidofovir, has been tried at much lower dosages than is used for cytomegalovirus infections, but these show little improvement since BK virus does not utilize ATP transferases in its replication cycle nor does it contain typical viral drug targets such as thymidine kinase or viral DNA polymerases (BKV uses the host cell factors present[10]).

Like other polyomaviruses, the BK virion is made of 360 copies of the major capsid protein VP1 that form 72 pentamers, each having a single minor capsid protein, VP2 or VP3, at its core. The VP1 monomer consists of antiparallel β-strands that fold into a jelly roll β-barrel structure with multiple exposed outer loops that nestle tightly with the adjacent monomer. To facilitate infection, BK virus utilizes its viral coat protein (VP1) to adhere to cells before it is endocytosed via cholesterol-dependent, caveola-mediated mechanisms. It is known that

Received: May 17, 2012
Revised: September 19, 2012
Published: September 24, 2012

dx.doi.org/10.1021/bi300639d | *Biochemistry* 2012, 51, 8092−8099

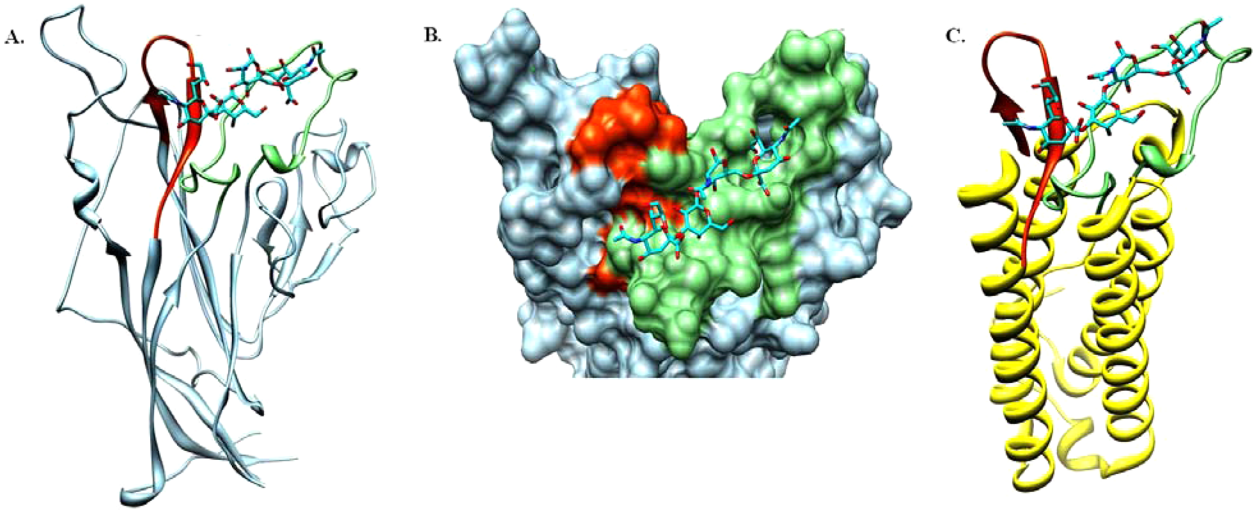

Figure 1. Carbohydrate binding site in VP1 of BKV. All panels show the HI loop colored orange and BC loop colored in green. (A) A homology model showing the interaction between NeuNAc-(α2,6)-Gal-(β1,3)-GlcNAc and the BC and HI loops of monomeric VP1 that are predicted to have a role in receptor binding.[12] (B) Top view in a space-filling model showing NeuNAc-(α2,6)-Gal-(β1,3)-GlcNAc in the binding groove formed by BC and HI loops in BKV VP1. (C) A model depicting the TM1526 4-helix protein bundle (yellow) superimposed onto BC and HI loops of BKV VP1 representing the design concept for final BKV BC/HI protein template.

Chart 1

M K V S D I L T V A I R L E E E G E R F Y R E L S E H F N G E I K K

T F L E L A D Q E R I H A E I F R K M S D Q E N W D E V D S Y L A G

Y A F Y E V F P D T S E I L R R K D L T L K E V L D I A I S V E K D S

I I L Y Y E L K D G L V N S D A Q K T V K K I I D Q E K E H L R K L

L E M K R E S T *

BKV VP1 uses an N-linked glycoprotein with α(2,3)-linked sialic acid as its receptor when binding to mammalian cells—specifically disialosyl-*N*-tetraglycosylceramide (GD1b) and trisialosyl-*N*-tetraglycosylceramide (GT1b).[11,21] Following this discovery, efforts were made to define the binding sites of the virus to its receptor as one possible target for the development of a BKV inhibitor.

Although there is currently no high-resolution structural data for the BKV VP1 pentamer, there is a structure of the JC virus[23] coat protein, which shares about 80% homology with BKV. Targeted mutagenesis studies coupled with molecular dynamics simulation of the VP1 of JCV have shown that the sialoganglioside receptor can stably interact with a groove found between the HI and BC loops.[12] These loops exist on the external surface of the coat protein and were identified using the crystal structure of mPyV in complex with a sialic acid receptor fragment as a guide to determine homologous amino acids on the JCV VP1.[16] In Figure 1, the homology model of the BKV VP1 monomer bound to a sialic acid glycan is shown, suggesting a role of the BC and HI loops.

Given the role of the extracellular loops of BKV VP1 in glycan binding, we examined the possibility of grafting the BC and HI loops onto a small protein that maintains the topological orientation of the wild-type VP1 and affords enhanced solubility, thermal stability, and facile incorporation of fluorescent tags. To this end, we decided to use TM1526—a four-helical protein bundle obtained from the thermophilic archaea bacteria *Thermatoga maritima* that is identical to Thermatoga rubrerythrin, an iron binding protein found within this species.[19] Based on an analysis of the crystal structure (PDB ID: 1JVX), TM1526 contains helices that are uniquely positioned such that grafted loops of the BKV binding determinants would maintain the topological orientation of wild-type BKV VP1. Here, we demonstrate that this engineered template binds to host cells in a dose-dependent manner that is abolished with an R64A mutation in the BC loop—results commensurate with wild-type virus experiments previously reported.[17] We also demonstrate that this template binds in a neuraminidase-dependent manner. Finally, we show that our template directly associates with sialogangliosides, GT1b and GD1b, to a similar extent as wild-type BKV VP1. Taken together, these results demonstrate the development of a novel protein template that mimics BK viral coat protein binding to cells.

EXPERIMENTAL PROCEDURES

Homology Modeling. The amino acid sequence of the BK virus was threaded through the X-ray structure of the JC virus (PDB code: 3NXG) using SwissModel. The resulting structure was subjected to extensive energy minimization and molecular dynamics as detailed elsewhere.[17] The BC and HI loops were then excised and grafted onto the X-ray structure of TM1526 (PDB code: 1VJX). The resulting model of the BK template is illustrated in Figure 1, with the BC and HI loops highlighted in green and orange, respectively.

Designing the BKV Template. The four-helix bundle template was derived from the ferritin-like diiron-carboxylate protein (TM1526) of *Thermotoga maritima*. The protein

dx.doi.org/10.1021/bi300639d | *Biochemistry* 2012, 51, 8092−8099

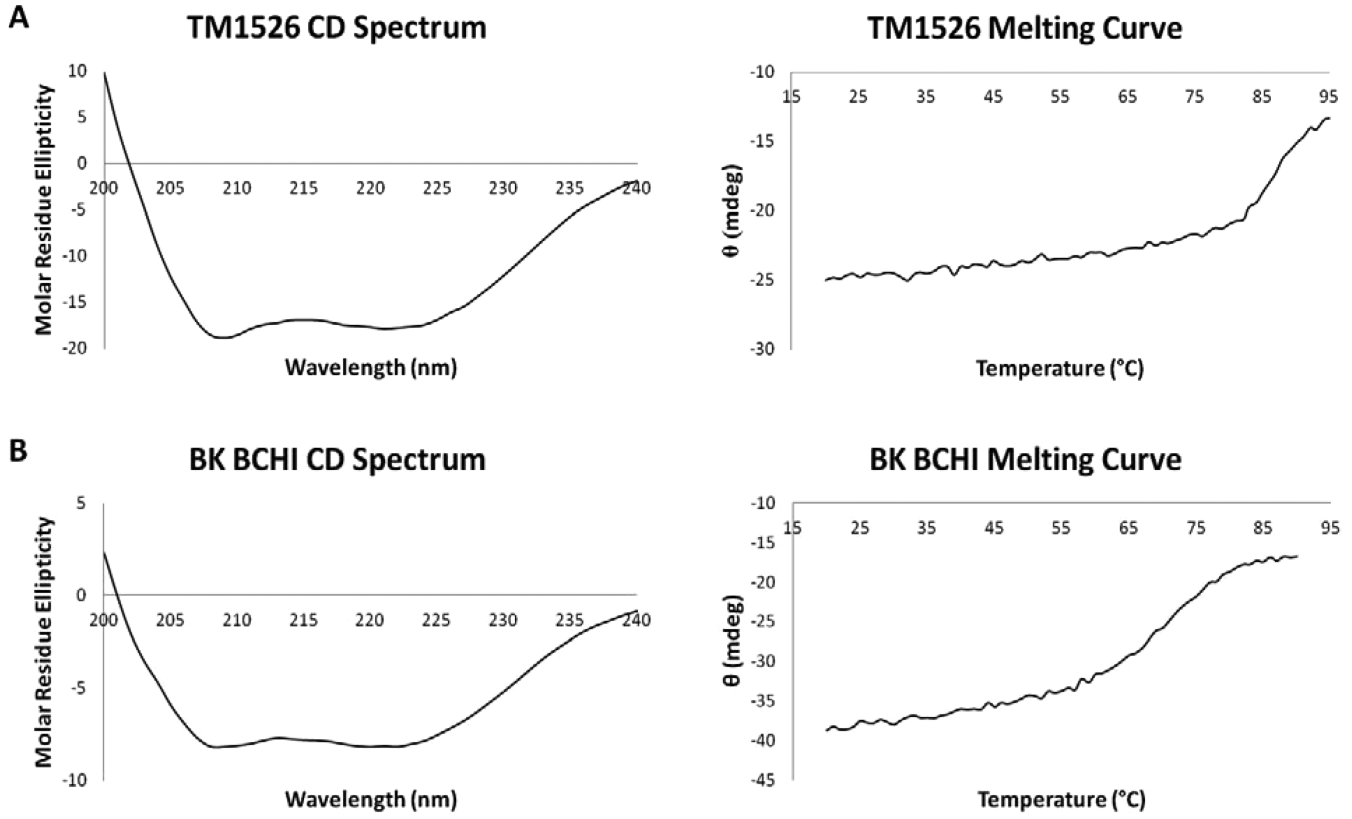

Figure 2. Characterizing the 4-helix template. (A) Circular dichroism and thermal melting curve of TM1526 template (10 μM) in PBS at pH 7.4 showing melting temperature of 85 °C. (B) Circular dichroism study and thermal melting curve of BKV BC/HI template (25.0 μM) in PBS at pH 6.8 showing a melting temperature of ~70 °C.

sequence is shown in Chart 1. The underlined segments identify the four α-helices in their native order. The residue sequences for the BK viral BC and HI loops are MGDPDENLRGFSLKLSAENDFSSDSPERKMLP and LFTNSSGTQQWRGL, respectively. Helices 3 and 4 were genetically engineered such that their adjoining loop was exposed on the same surface as the adjoining loop between helices 1 and 2 in native TM1526. This necessitated removal of the unstructured pass between helices 2 and 3 in native TM1526. These native loops connecting helices 1−2 and 3−4 were then replaced by the BC and HI loops from BKV VP1, respectively. A schematic depicting the template's protein engineering design is shown in Supporting Information Figure 1. To examine the importance of the smaller HI loop, a BC/BC template, containing two BC loops, was created. Additionally, the WDEV peptide sequence at the end of helix 2 in TM1526 was replaced with a GSGS sequence using the following primer: (5′-3′): ATAAAGATGTCAGACCAGGAAAACGGGTCTGGGTCGGATTCTAATTCCGATGCACAGAAA. The DNA sequence for the GSGS amino acid residues is underlined. The clones were produced by site-directed mutagenesis using Stratagene's QuikChange Lightning Site Directed Mutagenesis Kit protocols. All DNA sequencing, from this point forward, was performed at the Dartmouth College Sequencing Core Facility. Successfully mutated DNA constructs were transformed into BL21(DE3) *E. coli* cells (Invitrogen) for optimal protein production.

Mutating R64 Residue in BC Loop. Mutation of the R64 residue was achieved using Stratagene's QuikChange Lightning Site Directed Mutagenesis Kit. The following primer was used: (5′-3′): GATCCAGATGAGAACCTGGCCGGTTTCAGCCTCAAGCTG (R64A). The DNA sequence for the R64 residue mutation is underlined. Successful mutagenesis was confirmed by sequencing plasmid DNA with subsequent transformation into BL21(DE3) Star *E. coli* cells (Invitrogen).

Protein Production and Purification. *E. coli* cells were grown in Terrific Broth (TB) at 37 °C with shaking at 220 rpm until the optical density of the culture at 600 nm was above 0.6. The cultures were then induced with 1 mM IPTG. 1 mM $MgSO_4$ and 1 mL of ultrapure glycerol were added, and the cells were grown at 18 °C overnight. Pelleted cells were subsequently redissolved into 50 mL of lysis buffer (50 mM NaH_2PO_4, 300 mM NaCl, 10 mM imidazole, pH 8.0), 1 EDTA-free protease tablet (Roche), 2 μL of benzonase (250 U/μL, Sigma-Aldrich), and 2 mM $MgCl_2$ solution. The resulting suspension was applied to French press for lysis at 15 000 psi and then pelleted. The supernatant was filtered through a 0.45 μm filter and applied to a 5 mL HisTrap HP zinc affinity column utilizing gradual gradient elution on an Amersham Biosciences AKTAxpress fast protein liquid chromatography (FPLC). Protein elution was monitored by UV at a wavelength of 280 nm. All BKV protein templates eluted at ~30% of the elution buffer (50 mM NaH_2PO_4, 300 mM NaCl, 500 mM imidazole, pH 8.0). The fractions obtained were assessed using SDS-PAGE on 12% polyacrylamide MOPS NuPAGE gels, and the cleanest fractions were pooled. Pooled protein samples were further concentrated and then applied onto GE HiLoad Superdex75 16/60 size exclusion column for final purification. The purity of the protein sample was reassessed by SDS-PAGE. All template proteins eluted as dimers (~80%) and oligomers (~20%) (Supporting Information Figure 2). The fractions containing the dimers were

dx.doi.org/10.1021/bi300639d | *Biochemistry* 2012, 51, 8092−8099

pooled, concentration determined by UV, and stored in 5 mL aliquots at −80 °C. All UV readings for protein concentration were carried out on a Beckman Coulter DU800 spectrophotometer.

Assessing 4-Helix Template Stability. All circular dichroism experiments were carried out on a Jasco J-815 spectrometer (cell path length 0.1 cm). The absorbance was converted to residue molar ellipticity (θ) using standard conversion equation.[25] The percentage of secondary structure was calculated from the residue molar using the K2D2 algorithm as previously described.[22]

^{1}H NMR Spectroscopy. All ^{1}H NMR studies were performed on a Bruker 600 MHz spectrometer equipped with a cryoprobe and pulse field gradients. A total of 128 scans were acquired for each experiment with the BKV proteins and 1064 scans with JCV VP1. Data acquisition and processing were performed with TopSpin software (Bruker) running on a Linux workstation. One-dimensional spectra of proteins (BKV BC/HI, BKV VP1, and JCV VP1) with gangliosides (GT1b and GD1b) were acquired in 50 mM NaH_2PO_4, 150 mM NaCl, in 100% D_2O at pH 7.9. Experiments were performed using a protein to ganglioside ratio of 1:10. All experiments were run at 298 K.

Cells, Virus, and Antibodies. Vero cells (ATCC, VA) were maintained in a humidified 37 °C CO_2 chamber in minimal essential medium (MEM) (Mediatech, VA) supplemented with 1% penicillin/streptomycin solution (Mediatech, VA) and 5% heat-inactivated fetal bovine serum (Atlanta Biologics). The Dunlop strain of BKV Gardner (ATCC, VA) was propagated in Vero cells as previously described.[13] The monoclonal antibody mab416 (Oncogene, Cambridge, MA) detects the N-terminal portion of BKV large T antigen (T-ag) and was used for immunofluorescent staining of BKV infected cells.

Virus Propagation, Purification, and Labeling. BKV was propagated and purified as previously described.[14] To label BKV, fluorochrome conjugation with 20 μg/mL Alexa Fluor 488 carboxylic acid−succinimidyl ester (AF488) was added to purified BKV, and excess fluorescence was removed according to the manufacturer's labeling procedure (MP00143; Molecular Probes).

Flow Cytometry. Vero cells were harvested using CellStripper (Cellgro) following the manufacturer's protocol. Cells were spun for 5 min at 1500 rpm and washed twice in 1× PBS. 2.5 × 10^6 cells per sample were used. Cells were treated with PBS or 0.025 U/mL neuraminidase (NA) (Sigma) at 37 °C for 1 h. NA at 0.025 U/mL selectively cleaves α(2,3)-linked sialic acid.[11] Following NA treatment cells were spun for 5 min at 1500 rpm and washed twice in 1× PBS to remove cleaved sialic acid. Cells were then incubated with the indicated dose of GFP-labeled template or AlexaFluor-488-labeled BKV at 4 °C for 1 h. Cells were then spun and washed twice in PBS to remove unbound virus or template, fixed in 1% PFA, and fluorescence intensity was measured by flow cytometry (BD FacsCaliber).

RESULTS

Engineering the 4-Helix Template. The cytosolic, 4-helical bundle protein from *Thermatoga maritima*, TM1526, was used as a starting template largely due to its thermal stability, as evidenced by circular dichroism melting studies (Figure 2A), high solubility in aqueous buffer, its robust overexpression in nonpathogenic *E. coli* cells, and the availability of a high resolution X-ray structure (PDB code: 1VJX). We proceeded to modify this template using standard DNA cloning techniques in order to substitute the native loops found between helices 1−2 and 3−4 in native TM1526 with the relevant BC and HI loops of BKV VP1 (Figure 2B), respectively. To remove the unstructured pass between helices 2 and 3, and to orient the loops so that they exist on the same face of the helical bundle, the N-terminal end of helix 4 in TM1526 was ligated to the C-terminal end of helix 2, with replacement of the helical WDEV sequence coming of helix 2 with GSGS to provide a more flexible linker. The HI loop was used to connect the C-terminus of helix 4 and N-terminus of helix 3. This afforded the final template with its N- and C-termini on the same side of the helical bundle and the desired loops on the opposite face. A 6x His tag was incorporated into the N-terminus of the template to aid affinity purification. These modifications are detailed in Supporting Information Figure 1. Circular dichroism studies reveal a stable template with a melting temperature well above 37 °C at pH 6.8 (Figure 2B). The percent α-helicity is identical to that of native TM1526 at 84%, as determined by the K2D2 algorithm.[22]

Binding of GT1b and GD1b to the 4-Helix Template. One-dimensional ^{1}H NMR experiments were used to compare the direct binding of GT1b and GD1b, gangliosides previously shown to bind to the BK virus,[21] to the template and BKV VP1 pentamers. The gangliosides, with a tendency to form micelles, were kept below the reported CMC value of ∼100 μM,[24] with a concentration of 80 μM for GT1b and GD1b used, respectively. As evidenced by the line broadening of the ganglioside (Figure 3A), GT1b binds to the template at a ratio of 10:1 (ganglioside:protein) with a signal intensity reduction of 58.6% for the NH-acetyl protons at 1.754 ppm.[30] In accord with published reports of the ganglioside binding to the BKV virus, we observe similar GT1b binding to the BKV VP1 pentamer (Figure 3B) also at a ratio of 10:1, ganglioside:protein, with a signal intensity reduction of 65.5% for the NH-acetyl protons. As a control, we examined the binding of these gangliosides to the related JC virus VP1 pentamer. As shown in Figure 3C, there is no line broadening observed in the ^{1}H NMR spectrum.

Assessing Template Binding to Vero Cells in Vitro. Flow cytometry using GFP-tagged templates were conducted against Vero cells at increasing concentrations of template. A dose-dependent binding was observed for the BKV BC/HI template and BKV VP1. This dose dependence is reduced with the BKV BC/BC template and abolished with the BKV BC/HI R64A mutant (Figure 4). The treatment of the cells with neuraminidase, which removes sialic acid residues from cell surface proteins, significantly reduces the binding of the BC/HI template to the cells ($p < 0.05$; Figure 5).

DISCUSSION

Polyoma virus associated nephropathy is a serious clinical problem, leading to allograft dysfunction and transplantation loss. Current treatment management centers on early diagnosis and reduction of immunosuppressant therapy.[20] Although there are reports that targeting the BKV large T-antigen ATP-binding site might serve as a target for drug discovery,[18] this approach would require enhanced specificity against this ATPase which could be challenging particularly given the ubiquity and high variation of ATPases in the human body. We hypothesize that the rate of BKV infection can be curbed by competitively preventing viral binding to cells. While it can be expressed

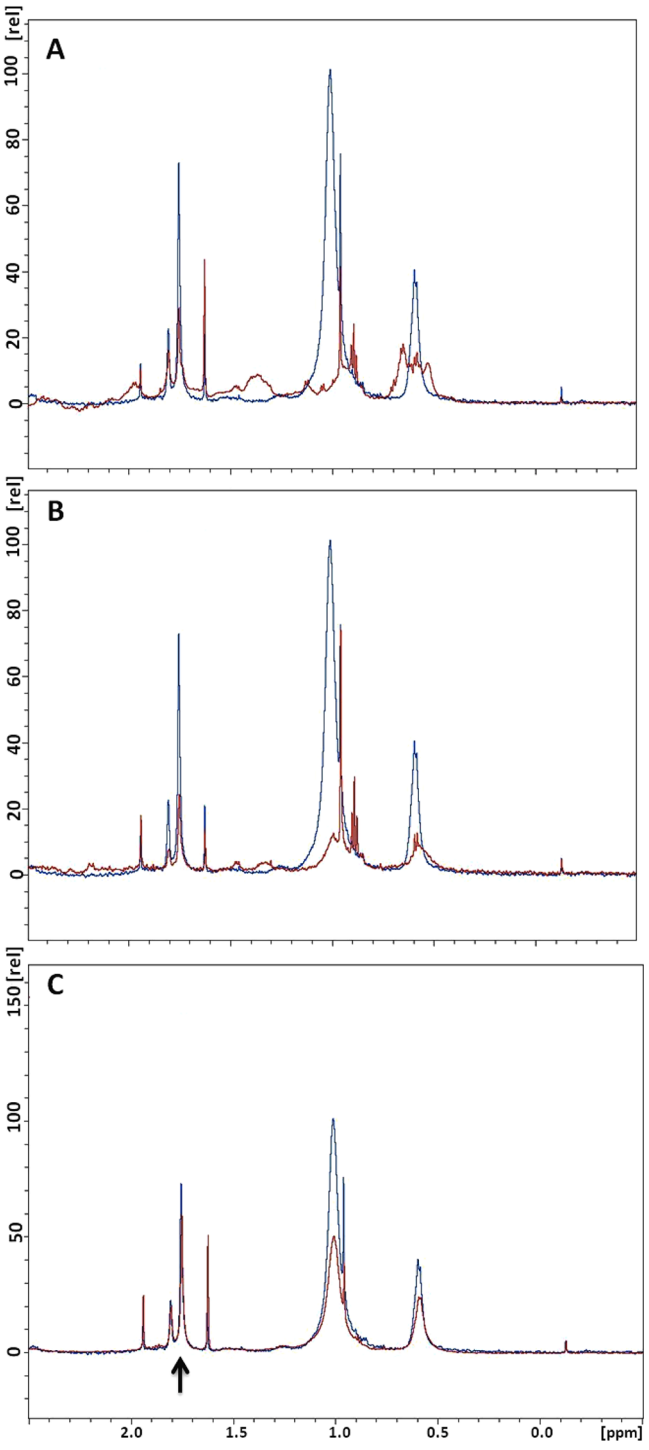

Figure 3. One-dimensional ^{1}H NMR of trisialoganglioside GT1b with protein. All spectra were obtained in buffer consisting of 50 mM NaH_2PO_4, 150 mM NaCl, 100% D_2O, pH 8.0. In all overlays shown, the blue spectrum is GT1b in buffer alone (control) and shows the 1D ^{1}H NMR spectra of 80 μM GT1b in buffer and the red spectrum shows the respective proteins (all at 8 μM) with which GT1b was incubated. Only the aliphatic region (0−2.5 ppm), highlighting regions of methylene and methyl groups, is shown. (A) BKV BC/HI protein template interacting with GT1b. (B) BKV VP1 incubated with GT1b. (C) JCV VP1 incubated with GT1b (the difference in peak intensity can be attributed to a larger number of scans collected for the JCV VP1, required to obtain adequate signal-to-noise ratios).

recombinantly, BK viral coat protein is a large molecular weight pentamer difficult to manipulate for screening methodologies, particularly those requiring fluorescent tags. To this end, we sought to develop a smaller protein template that recapitulates the binding determinants of native BKV VP1 as a potential tool for identifying molecular inhibitors against BK virus.

Because of its robust recombinant overexpression, thermal stability, relatively small size, and favorable solubility properties, a four-helical protein bundle derived from the thermophilic archaea *Thermatoga maritima* was chosen as a starting template (Figure 1) for replicating the binding properties of native BKV VP1. Based on circular dichroism results, the predominantly helical content of the parent TM1526 was maintained in our protein template (Figure 2B). This conformation is critical because the proximity of the binding loops to recapitulate the pocket seen in native BKV VP1 (as modeled in Figure 1) is dependent on this structural integrity. Rearrangement of the helices, including removal of the unstructured pass, led to a template with reduced thermal stability (data not shown). Closer analysis revealed that the remaining loop between helices 2 and 4 contained the helical WDEV sequence of wild-type TM1526, thereby possibly restricting the formation of a stable 4-helical bundle. Replacement of these residues with two alternating glycine−serine residues, GSGS, thereby allowing for more flexibility, improved the thermal stability of the template, as shown by the circular dichroism melting results of Figure 2B.

The ability of our template to directly bind to the GT1b and GD1b sialogangliosides, reported to bind to BKV,[21] was ascertained by a series of 1D ^{1}H NMR studies (Figure 3). These sialogangliosides have been found as receptors on the surface of mononuclear cells[27] and also on cortical tubular and medullary tissue[28] and have been implicated in erythrocyte hemaglutination seen as a result of BKV infection. This activity is sensitive to neuraminidase treatment, which removes the terminal sialic acid of many gangliosides and glycoproteins.[29] The ^{1}H NMR experiments demonstrate that both sialoganglio-sides bind to our template at a ratio of 10:1, sialoganglioside:-protein, as evidenced by the extensive line broadening. To quantitate the line broadening observed, the large methyl peak at 1.01 ppm was set to a relative value of 100, and the percent peak intensity reduction of the NH-acetyl protons (1.754 ppm, indicated by arrow in Figure 3) present on the sialic acid moieties of the gangliosides were calculated. The percent peak intensity reduction of the BKV BC/HI template and BKV VP1 were 58.6% and 65.5%, respectively. The slight difference in peak reduction can be attributed to the larger size of BKV VP1 and its pentameric nature, affording it more binding sites for the sialogangliosides compared to the BKV BC/HI template. As expected, the JCV VP1 pentamer does not bind to either GT1b or GD1b upon 1D ^{1}H NMR studies (Figure 3C), a result that is in agreement with the recent report that JCV VP1 binds only to NeuNAc-α2,6-Gal-β1,4-GlcNAc-β1,3-Gal-β1,4-Glc (LSTc) upon screening of a glycan array.[23]

Within the homology model of the BKV VP1, the BC loop plays a predominate role in ligand binding, yielding a concaved structure that forms two loops (denoted BC1 and BC2) surrounding the ligand.[15,16] In addition, the BC loop (34 residues) is significantly longer than the HI loop (14 residues). We therefore examined a template containing two BC loops to determine the contributions of the individual loops. In Figure 4, using GFP-tagged versions of our engineered template, flow cytometry data are presented showing dose-dependent binding of BKV VP1 and BKV BC/HI to Vero cells. In this assay, we

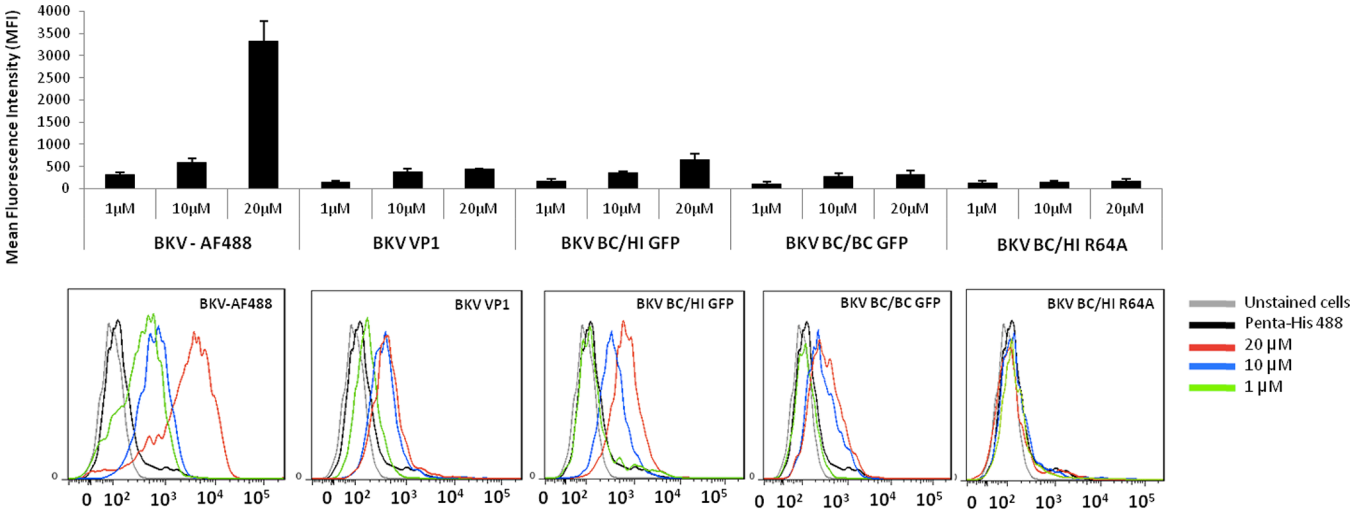

Figure 4. Dose-dependent binding of BKV templates and BK virus to Vero cells. Vero cells were harvested and incubated with the indicated dose of Alexa-Fluor 488-labeled BKV (BKV-AF488), BKV VP1, or template at 4 °C for 1 h. Following binding, samples were washed in PBS and fixed in 1% paraformaldehyde (BKV-AF488, BC/BC-GFP, and BC/HI-GFP) or incubated an additional hour at 4 °C with secondary antibody (BKV VP1, BC/HI-R64A) (Qiagen, Penta-his 488). Samples were analyzed for binding by flow cytometry (BD FACSCaliber, FlowJo analysis software; $N = 3$).

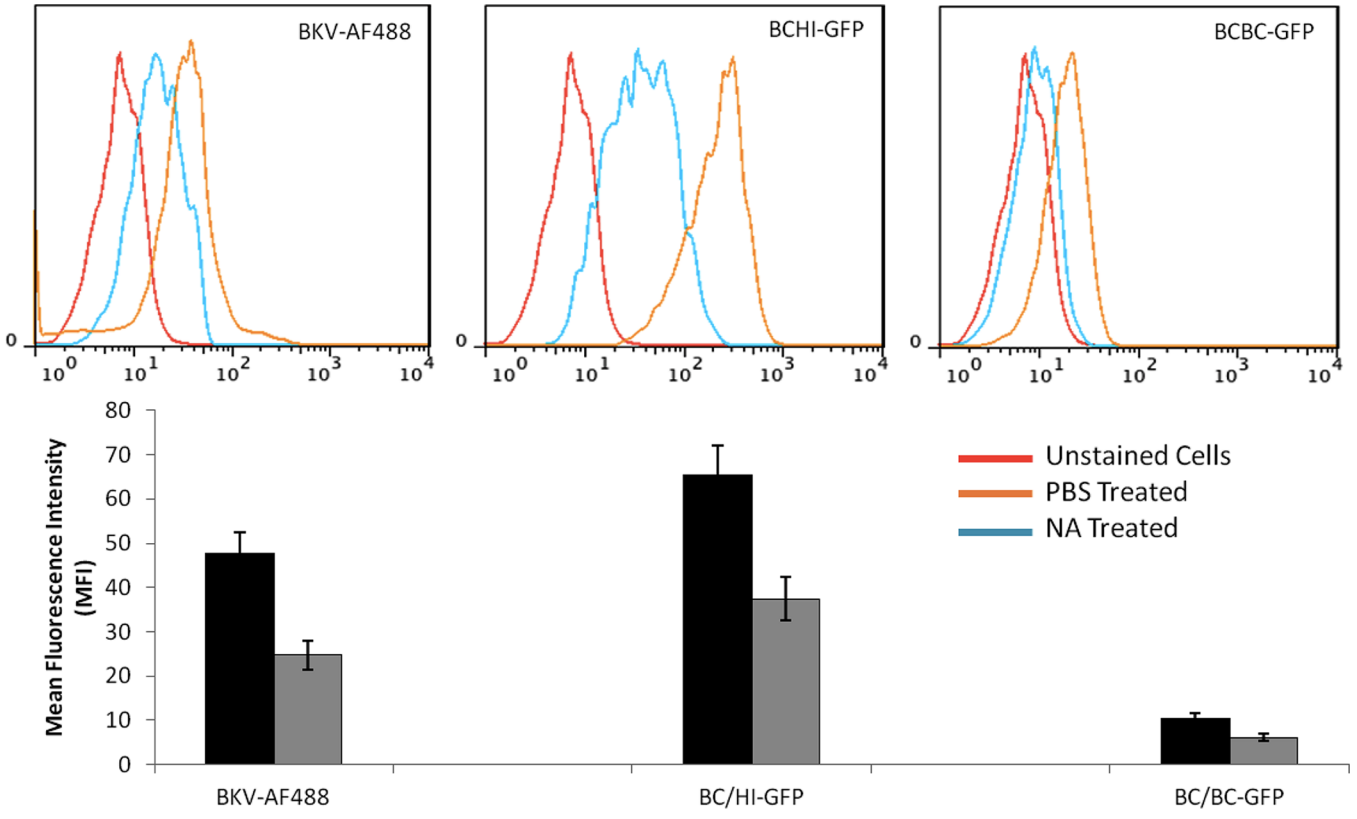

Figure 5. Flow cytometry of GFP tagged BKV templates using neuraminidase (NA) treated cells. In top panel, Vero cells were incubated with PBS or NA, washed with PBS, and incubated with Alexa-Fluor 488-labeled BKV (BKV-AF488; $p = 0.010$), GFP-tagged BKV BC/HI mutant ($p = 0.025$), or GFP-tagged BKV BC/BC mutant ($p = 0.164$). Red line represents unstained cells. Following binding, cells were washed in PBS and analyzed by flow cytometry. The bottom panel shows MFI of PBS treated (black) and neuraminidase treated (gray) Vero cells, bound with BKV and BKV-VP1 template.

observe a reduction in the binding capacity of the BKV BC/BC version of our template, signifying the importance of the incorporated HI loop, and an abolishment of dose dependence with the R64A mutation in the BC loop—a result in corroboration with previous reports employing the complete virus.[17] In this figure, it is evident that the wild-type virus control binds more strongly to Vero cells than either pentameric BKV VP1 or our BKV BC/HI template at 20 μM. This reflects the wild-type virus' avidity afforded by the multivalency of the full coat, which gives it an advantage in binding to cells. Nevertheless, as the building unit of the full viral coat, the VP1 protein is pivotal to inhibitor development

dx.doi.org/10.1021/bi300639d | *Biochemistry* 2012, 51, 8092−8099

efforts, and our goal here was to replicate the binding capability of this protein with our engineered template mimic. To this end, Figure 4 shows that there is comparable binding affinity to cells between our BKV BC/HI template and the VP1 protein. When cells were incubated with neuraminidase, we observe a significant 40% reduction in the binding capacity of our BKV BC/HI template—a degree commensurate with that seen with BK wild-type virus ($p < 0.05$; Figure 5). The BKV BC/BC construct does not display as marked a difference in cellular binding in the presence or absence of neuraminidase treated cells ($p = 0.164$). Taken together with Figure 4, these results suggest that our BKV templates bind to cells utilizing the grafted viral loops and that the HI loop, though considerably smaller than the BC loop, plays a necessary role in this binding event.

Attempts to reduce viral infectivity in the presence of BKV VP1 protein and BKV BC/HI template showed statistically insignificant reduction with both protein samples (data not shown). We attribute this result to the multivalent nature of the full wild-type viral coat which, as described above, exhibits a much higher avidity to cell receptors than our BC/HI template or VP1 pentamer. Herein lies the challenge and the motivation to find an effective small molecule drug treatment against PVAN that can combat the enhanced cellular binding seen with the wild-type BK viral coat. We believe that the small size, thermal stability, and solubility of the BKV BC/HI template mimicking the cellular binding properties of the pentameric building unit of the BK viral coat detailed in this report may provide a tool to further future drug screening efforts, as well as facilitate structural characterization of the interaction of BKV with its cognate receptor.

■ ASSOCIATED CONTENT

Supporting Information

Details of protein engineering the 4-helix template and representative protein template purification profile. This material is available free of charge via the Internet at http://pubs.acs.org.

■ AUTHOR INFORMATION

Corresponding Author

*Tel (603) 646-1154; Fax (603) 646-3946; e-mail dale.mierke@dartmouth.edu.

Funding

This work was supported by the National Institutes of Health grant P01-NS065719 to D.F.M.

Notes

The authors declare no competing financial interest.

■ ACKNOWLEDGMENTS

We thank Dr. Gabriel Gaidos (Dartmouth College) for critical discussions and experimental guidance during the course of this work and Dr. Edward Hawrot (Brown University) for providing the cDNA for *Thermatoga maritima*.

■ ABBREVIATIONS

BKV, BK virus; PVAN, polyoma virus associated nephropathy; GFP, green fluorescent protein; VP1, viral coat protein 1; IPTG, isopropyl-β-D-thiogalactopyranoside; FPLC, fast protein liquid chromatography; PFA, paraformaldehyde; BKV BC/HI, BK viral coat protein mimic employing the BC and HI loops of BK virus on TM1526 protein; BKV BC/BC, BK viral coat protein mimic employing two BC loops on TM1526 protein; NA, neuraminidase; PBS, phosphate buffered saline; CMC, critical micellar concentration; GT1b, trisialosyl-*N*-tetraglycosylceramide; GD1b, disialosyl-*N*-tetraglycosylceramide; MFI, mean fluorescence intensity; IL-2, interleukin 2; JCV, John Cunningham virus; mPyV, murine polyoma virus.

■ REFERENCES

(1) Hirsch, H. (2005) BK virus: Opportunity Makes a Pathogen. *Clin. Infect. Dis. 41*, 354−360.

(2) Bonvoisin, C., Weekers, L., Xhignese, P., Grosch, S., Milicevic, M., and Krzesinski, J.-M. (2008) Polyomavirus in Renal Transplantation: A Hot Problem. *Transplantation 85* (supplemental), 42−48.

(3) Cimbaluk, D., Pitelka, L., Kluskens, L., and Gattuso, P. (2009) Update on Human Polyomavirus BKV Nephropathy. *Diagn. Cytopathol. 37*, 773−779.

(4) Nickeleit, V., Singh, H., and Mihatsch, M. (2003) Polyomavirus Nephropathy: Morphology, Pathophysiology, and Clinical Management. *Curr. Opin. Nephrol. Hypertens. 12*, 599−605.

(5) Loeches, B., Valerio, M., Perez, M., Banares, R., Ledesma, J., Fogeda, M., Saledo, M., Rincon, D., Bouza, E., and Munoz, P. (2009) BK Virus in Liver Transplant Recipients: A Prospective Study. *Transplant. Proc. 41*, 1033−1037.

(6) Brennan, D., Agha, I., Bohl, D., Schnitzler, M., Hardinger, K., Lockwood, M., Torrence, S., Schuessler, R., Roby, T., Gaudreault-Keener, M., and Storch, G. (2005) Incidence of BKV with Tacrolimus versus Cyclosporine and Impact of Preemptive Immunosuppression Reduction. *Am. J. Transplant. 5*, 582−594.

(7) Randhawa, P., Farasati, N., Shapiro, R., and Hostetler, K. (2006) Ether Lipid Ester Derivatives of Cidofovir Inhibit Polyomavirus BK Replication In Vitro. *Antimicrob. Agents Chemother. 50*, 1564−1566.

(8) Bernhoff, E., Tylden, G., Kjerpeseth, L., Gutteberg, T., Hirsch, H., and Rinaldo, C. (2009) Leflunomide Inhibition of BK Virus replication in Renal Tubular Epithelial Cells. *J. Virol. 84*, 2150−2156.

(9) Araya, C., Garin, E., Neiberger, R., and Dharnidharka, V. (2010) Leflunomide Therapy for BK Virus Allograft Nephropathy in Pediatric and Young Adult Kidney Transplant Recipients. *Pediatr. Transplant. 14*, 145−150.

(10) Sriaroon, C., Greene, J., Vincent, A., Tucci, V., Kharfan-Dabaja, M., and Sandin, R. (2010) BK Virus: Microbiology, Epidemiology, Pathogenesis, Clinical Manifestations and Treatment. *Asian Biomed. 4*, 3−18.

(11) Dugan, A., Eash, S., and Atwood, W. (2005) An N-linked Glycoprotein with alpha(2,3)-linked Sialic Acid is a Receptor for BK Virus. *J. Virol. 79*, 14442−14445.

(12) Gee, G., Dugan, A., Tsomaia, N., Mierke, D., and Atwood, W. (2006) The Role of Sialic Acid in Human Polyomavirus Infections. *Glycoconjugate J. 23*, 19−26.

(13) Raptis, L. (2001) *SV40 Protocols*, Humana Press Inc., Totowa, NJ.

(14) Eash, S., Querbes, W., and Atwood, W. (2004) Infection of Vero Cells by BK Virus is Dependent on Caveolae. *J. Virol. 78*, 11583−11590.

(15) Stehle, T., and Harrison, S. (1997) High Resolution Structure of a Polyomavirus VP1-oligosaccharide Complex: Implications for Assembly and Receptor Binding. *EMBO J. 16*, 5139−5148.

(16) Gee, G., Tsomaia, N., Mierke, D., and Atwood, W. (2004) Modelling a Sialic Acid Binding Pocket in the External Loops of JC Virus VP1. *J. Biol. Chem. 47*, 49172−49176.

(17) Dugan, A., Gasparovic, M., Tsomaia, N., Mierke, D., O'Hara, B., Manley, K., and Atwood, W. (2007) Identification of Amino Acid Residues in BK Virus VP1 that are critical for Viability and Growth. *J. Virol. 81*, 11798−11808.

(18) Zeng, G., Bueno, M., Camachos, C., Ramaswami, B., Luo, C., and Randhawa, P. (2009) Validation of BKV Large T-antigen ATP-Binding Site as a Target for Drug Discovery. *Antiviral Res. 81*, 184−187.

(19) Joint Center for Structural Genomics (JCSG) Crystal Structure of Putative Ferritin-like Diiron-Carboxylate Protein (TM1526) from *Thermotoga maritima* at 2.30 resolution. To be published 4/1/04.
(20) Hardinger, K., Koch, M., Bohl, D., Storch, G., and Brennan, D. (2010) BK Virus and the Impact of Pre-emptive Immunosuppression Reduction: 5-year Results. *Am. J. Transplant. 10*, 407−415.
(21) Low, J., Magnuson, B., Tsai, B., and Imperiale, M. (2006) Identification of gangliosides GD1b and GT1b as Receptors for BK Virus. *J. Virol. 80*, 1361−1366.
(22) Perez-Iratxeta, C., and Andrade-Navarro, M. (2008) K2D2: Estimation of Protein Secondary Structure from Circular Dichroism Spectra. *BMC Struct. Biol. 8*, 25−29.
(23) Neu, U., Maginnis, M., Palma, A., Stroh, L., Nelson, C., Feizi, T., Atwood, W., and Stehle, T. (2010) Structure-Function Analysis of the Human JC Polyomavirus Establishes the LSTc Pentasaccharide as a Functional Receptor Motif. *Cell Host Microbe 8*, 309−319.
(24) Ulrich-Bott, B., and Wiegandt, H. (1984) Micellar Properties of Glycosphingolipids in Aqueous Media. *J. Lipid Res. 25*, 1233−1240.
(25) Whitmore, L., and Wallace, B. (2004) DICHROWEB, an online server for protein secondary structure analyses from circular dichroism spectroscopic data. *Nucleic Acids Res. 32*, W668−673.
(26) Gardner, S., Field, A., Coleman, D., and Hulme, B. (1971) New Human Papovavirus (B.K.) Isolated from Urine After Renal Transplantation. *Lancet 297*, 1253−1257.
(27) Tsuboyama, A., Takaku, F., Sakamoto, S., Kano, Y., Ariga, T., and Miyatake, T. (1980) Characterization of Gangliosides in Human Leucocytes. *Br. J. Cancer 42*, 908−914.
(28) Holthofer, H., Reivinen, J., and Miettinen, A. (1994) Nephron Segment and Cell Type Specific Expression of Gangliosides in the Developing and Adult Kidney. *Kidney Int. 45*, 123−130.
(29) Sinibaldi, L., Donatelli, V., Goldoni, P., Cavallo, G., Vavoni, C., and Orsi, N. (1987) Inhibition of BK Virus Haemaglutination by Gangliosides. *J. Gen. Virol. 68*, 879−883.
(30) Ishida, H.-K., Ishida, H., Kiso, M., and Hasegawa, A. (1994) Total Synthesis of Ganglioside GQ1b and the related polysialogangliosides. *Tetrahedron: Asymmetry 5*, 2493−2512.